https://doi.org/10.5194/egusphere-2024-4079
Preprint. Discussion started: 15 January 2025

The global ocean mixed layer depth derived from an energy approach

Efraín Moreles[1], Emmanuel Romero[2], Karina Ramos-Musalem[3], and Leonardo Tenorio-Fernandez[4,5]

[1]Instituto de Ciencias del Mar y Limnología, Universidad Nacional Autónoma de México, Mexico City, Mexico
[2]Universidad Autónoma de Baja California Sur, Departamento Académico de Sistemas Computacionales, Carretera al sur km 55, Col. Mezquitito, La Paz, BCS, Mexico
[3]Department of Physical Oceanography, Centro de Investigación Científica y de Educación Superior de Ensenada, Ensenada, Baja California, Mexico
[4]Instituto Politécnico Nacional-Centro Interdisciplinario de Ciencias Marinas, Departamento de Oceanología. Av. Politécnico Nacional s/n. Col. Palo de Santa Rita, 23096, La Paz, Baja California Sur, Mexico
[5]CONHACyT, Consejo Nacional de Humanidades, Ciencia y Tecnología. Av. Insurgentes Sur 1582, Col. Crédito Constructor, Demarcación Territorial Benito Juárez, 03940, Mexico City, Mexico

Correspondence: Efraín Moreles (moreles@cmarl.unam.mx)

Abstract.

The mixed layer depth (MLD) is critical for understanding ocean-atmosphere interactions and internal ocean dynamics. Traditional methods for determining the MLD commonly rely on hydrographic thresholds that vary spatially and temporally with local oceanographic conditions, limiting their global consistency and applicability. To address this, we propose an energy-based methodology that defines the MLD as the depth at which the work done by buoyancy (WB) reaches 20 J m^{-3}. Based on the structural change in WB, the MLD criterion identifies the upper ocean's well-mixed layer in energetic terms. This approach provides a robust criterion based on physical principles, which is globally and temporally consistent and easy to implement. Our methodology aligns with turbulent boundary layer dynamics while maintaining quasi-homogeneity in density and temperature for most of the global ocean throughout the year. A global monthly MLD climatology derived from this method demonstrates its reliability across diverse oceanic conditions and its accuracy in regions and seasons where conventional methods struggle. Our study advances the development of MLD energy-based methodologies by providing a single energy value to define the MLD globally during all months. This energy-based approach could offer significant potential for advancing the study of dynamic, and thermodynamic processes, including heat content and vertical exchanges. It could also serve as a robust tool for validating ocean circulation models and to support intercomparison studies in initiatives such as the Ocean Model Intercomparison Project (OMIP) and the International Coupled Model Intercomparison Project (CMIP). Future research will explore its applicability to high-frequency processes and regional variability, further enhancing its utility for understanding and modeling oceanic phenomena.

https://doi.org/10.5194/egusphere-2024-4079
Preprint. Discussion started: 15 January 2025

1 Introduction

The ocean mixed layer is the ocean's surface layer in direct contact with the atmosphere, whose properties (potential density, temperature, salinity, and other tracers) are relatively homogeneous in the vertical. The mixed layer plays a crucial role in the Earth's weather and climate since it determines the energy, mass, and momentum exchanges between the ocean and the atmosphere (Gill, 1982). It largely determines different aspects of the climate system: ocean surface temperature (Deser et al., 2010), formation and properties of water masses (Hanawa and D.Talley, 2001; Groeskamp et al., 2019), thermal energy available to a tropical cyclone (Shen and Ginis, 2003), biological productivity (Franks, 2014; Bouman et al., 2020), chlorophyll content (Briseño Avena et al., 2020; Carvalho et al., 2017) and carbon subduction (Bopp et al., 2015; Omand et al., 2015). Consequently, the mixed layer depth (MLD) is a key variable in understanding the past, present, and future variability of Earth's weather and climate (Sallée et al., 2021; Reichl et al., 2022; Treguier et al., 2023).

The definition of the mixed layer as a relatively homogeneous layer is very vague (de Boyer Montégut et al., 2004), which has led to numerous definitions and estimates of the MLD (de Boyer Montégut et al., 2004; Holte and Talley, 2009; Schofield et al., 2015; Reichl et al., 2022; Romero et al., 2023). The above has resulted in high uncertainty in estimating the MLD, mainly in deep and intermediate water formation regions, polar seas, and barrier layer regions (Treguier et al., 2023). That also has affected the analysis of the relationship between the MLD and various ecological processes, such as chlorophyll-a content, phytoplankton dynamics, and primary production (Carvalho et al., 2017; Bouman et al., 2020). No MLD definition provides accurate estimates for all world regions under different ocean conditions throughout the year.

Different authors have suggested that the physically relevant definitions of MLD should be density-based since this approach captures both temperature and salinity-driven stratifications at the mixed layer (Griffies et al., 2016; Sallée et al., 2021; Treguier et al., 2023). The protocol used to compute the MLD in the Ocean Model Intercomparison Project (OMIP) and the International Coupled Model Intercomparison Project (CMIP) considers a constant density threshold; however, in regions with vertically compensated layers, the density threshold may overestimate the MLD (de Boyer Montégut et al., 2004). No physical reason sustains the choice of a specific density threshold; instead, it is heuristically obtained. Reichl et al. (2022) proposed a MLD definition considering the gravitational potential energy of the water column; while their work is promising because it is based on physical principles, further research is required to select the energy value that defines the MLD and investigate if such value is globally applicable during all seasons (Treguier et al., 2023).

Consequently, further work is needed to develop a methodology based on physical principles for calculating the MLD that provides accurate estimates for all world regions under different ocean conditions. Energy-based approximations for calculating the MLD need to be investigated in more detail to determine if a single energy value can determine the MLD globally during all seasons.

This study aims to develop a physics-based methodology, based on energy considerations, for calculating the MLD under different ocean conditions in all world regions. The methodology's global applicability is one of its crucial contributions. Based on the work done by the buoyancy force to vertically displace a water parcel, the homogeneity of the ocean's upper layer was quantified. Then, the value of this work, which determines the well-mixed upper layer and the MLD globally during all months,

https://doi.org/10.5194/egusphere-2024-4079
Preprint. Discussion started: 15 January 2025

was carefully investigated. Finally, an observation-based global MLD climatology was constructed, which could be a reference to validate numerical solutions and perform MLD model intercomparison studies. The energy-based definition of the MLD is consistent with physics and is easy to implement numerically; it has the potential to provide further insights into various dynamic (e.g., vertical exchanges within the ocean and between the ocean and the atmosphere), thermodynamic (upper ocean heat content), and ecological (e.g., chlorophyll-a content and phytoplankton dynamics) processes.

2 Methodology and data

2.1 An energy measure of the mixed layer depth

The relatively vertical homogeneity of the mixed layer is due to turbulence caused by wind effects, buoyancy-driven fluxes, and waves (D'Asaro, 2014; Sallée et al., 2021; Reichl et al., 2022). The mixed layer concept allows for diagnosing vertical exchanges within the ocean and those between the ocean and the atmosphere without a detailed analysis of the associated turbulent processes (D'Asaro, 2014; Sutherland et al., 2014; Franks, 2014; Reichl et al., 2022). Therefore, a quantitative measure of the vertical homogeneity of the upper ocean layer is needed to calculate the MLD.

Since vertical changes in density hinder turbulence and subsequent mixing, a physically relevant definition of the water column's vertical homogeneity should be density-based and derived from physical principles. The approach proposed here to quantify the water column's vertical homogeneity is based on energy considerations. It quantifies the work done by the buoyancy force to vertically displace a water parcel under static instability conditions, herein referred to as the work done by buoyancy (WB). By considering vertical displacements from the ocean's interior to the surface, WB can constitute a proxy for the vertical homogeneity of the water column: the higher the WB, the lower the vertical homogeneity of the water column, and vice versa.

Consider a fluid in hydrostatic balance in which a water parcel is adiabatically displaced along the vertical from level z to $z+\delta z$; in such a displacement the potential density is materially conserved. According to Vallis (2017), the parcel experiences a force (per unit volume) given by

$$\delta F = g\frac{d\rho^{\theta}(z)}{dz}\delta z, \tag{1}$$

where g is the acceleration of gravity and ρ^{θ} is the potential density referred to the pressure at level $z+\delta z$. From the above equation, the buoyancy force experienced by a parcel, initially at equilibrium at z_{eq}, when displaced from z_{eq} to any depth z is given by

$$F(z) = g\left[\rho^{\theta}(z) - \rho^{\theta}(z_{\text{eq}})\right]. \tag{2}$$

The force is null at z_{eq}, positive if $\rho^{\theta}(z) > \rho^{\theta}(z_{\text{eq}})$ and negative if $\rho^{\theta}(z) < \rho^{\theta}(z_{\text{eq}})$. By calculating the line integral of the buoyancy force along such a displacement, WB is obtained,

$$\text{WB}_{z_{\text{eq}}\to z} = \text{WB}(z) = \int_{z_{\text{eq}}}^{z} F(\gamma)d\gamma = -g\,(z - z_{\text{eq}})\,\rho^{\theta}(z_{\text{eq}}) + g\int_{z_{\text{ref}}}^{z}\rho^{\theta}(\gamma)d\gamma. \tag{3}$$

https://doi.org/10.5194/egusphere-2024-4079
Preprint. Discussion started: 15 January 2025

WB depends on the cumulative effect along the vertical of the buoyancy force, which in turn depends on the difference between ρ^{θ} at z_{eq} and any depth z.

In stable density profiles, where ρ^{θ} increases with depth, WB is negative for upward and downward displacements of the water parcel; the displaced water parcel tends to return to its original depth z_{eq} where it was at equilibrium. For an upward displacement (positive displacement), the force is downward; for a downward displacement (negative displacement), the force is upward. The opposite behavior is obtained in unstable density profiles, where ρ^{θ} decreases with depth.

The use of WB as a proxy for the vertical homogeneity of the water column can be exemplified by considering typical density profiles in different seasons (Fig. 1). The WB required to displace each water parcel in the water column from its equilibrium level to the surface is also shown for each density profile. There is a strong correspondence between the density profile and its associated WB profile: a water column homogeneous in density has zero or small WB values, whereas a stratified water column has density and WB increasing with depth. However, because WB is a nonlinear function of density, the density variation between two depths is not proportional to the corresponding increase in WB. The stratified and winter profiles in Fig. 1 show that large density variations do not always correspond to large WB values.

Since the mixed layer is defined as the upper ocean layer in direct contact with the atmosphere, it is expected that the water parcels can move with little or no energy within it. Consequently, WB is better than density for diagnosing the water column section in direct contact with the atmosphere and its vertical homogeneity in energetic terms. In this study, the mixed layer is defined as the upper ocean layer relatively homogeneous in WB (with small WB values), which is well-mixed in energetic terms and, therefore, in contact with the atmosphere. From the mixed layer definition, the MLD is thus the depth at which WB changes from zero or small values near the surface to values that considerably increase downward (the depth at which WB has a structural change). Different mathematical methods can be used to find the structural change in WB; in this study, we used the vertical gradient of WB (WB_z). However, for strongly stratified or very smooth density profiles, a clear structural change in WB is not easy to find; in these cases, it is useful to consider a specific WB threshold characterizing a homogeneous layer.

The depth of the structural change in WB (Fig. 1) depends on the corresponding density profile. For idealized density profiles with a strong and unique pycnocline (summer and winter profiles in Fig. 1), the MLD is clearly defined: the mixed layer corresponds to the upper section of the water column homogeneous in WB, in which no work is required to displace any water parcel from its equilibrium level to the ocean surface. For strongly stratified density profiles, profiles with several pycnoclines, or very smooth density profiles, the mixed layer can be shallow or deep depending on a chosen threshold characterizing homogeneous WB values. For the strongly stratified density profile in Fig. 1a, the mixed layer could be very shallow or non-existent. For the density profile with near-surface restratification in Fig. 1d, the mixed layer can be as shallow as 50 m, as deep as 200 m, or has other depths depending on a WB threshold characterizing a homogeneous section.

This new MLD definition is based on energy considerations and derived from physical principles. Thus, it can be considered adequate and applicable in different regions and oceanic conditions, such as polar seas, intermediate and deep water formation regions, and barrier and compensated layers. However, it is necessary to investigate the WB threshold that determines the MLD globally during all seasons, if there is one.

https://doi.org/10.5194/egusphere-2024-4079
Preprint. Discussion started: 15 January 2025

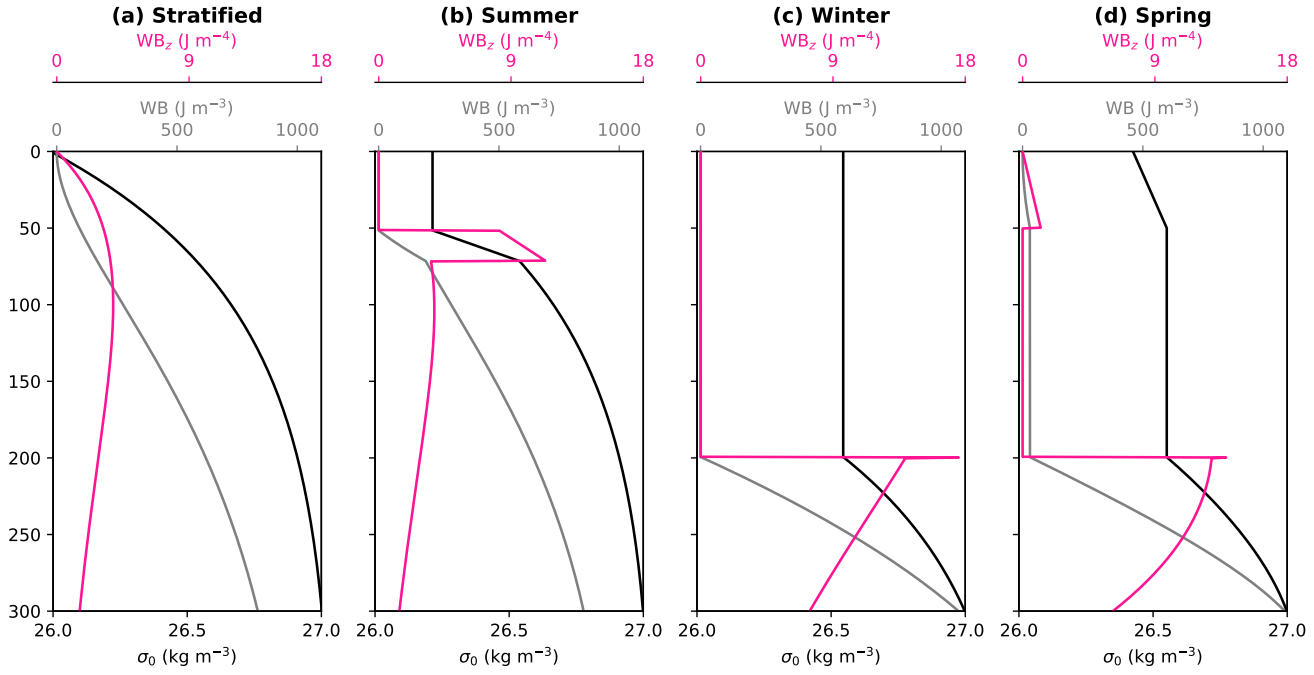

Figure 1. Typical density profiles in different conditions and seasons (black curves), the corresponding WB required to displace a water parcel from any depth to the surface (gray curves), and its associated vertical gradient WB_z (pink curves). The density profiles are the same as those used by Treguier et al. (2023) in their Fig. 2. The plots show the potential density anomaly σ_0, assuming that the potential density referred to 0 dbar was used.

2.2 Data

Two types of global-scale in situ data were used to analyze the MLD. The first dataset, from the World Ocean Circulation Experiment (WOCE), considered transects along the Pacific Ocean. These transects were used to investigate a WB value that could determine the MLD during all seasons. The second dataset, comprising Argo profiles for the global ocean (Wong et al., 2020), was used to construct an energy-based global monthly MLD climatology, further enhancing the applicability of this study.

2.2.1 WOCE data

Five transects in the Pacific Ocean were obtained from the WOCE (https://cchdo.ucsd.edu/, accessed in March 2024). The chosen transects cover the seasonal variation, except spring, of the hydrography throughout the Pacific Ocean:

- The meridional section transects P14S (67°S-10°S along the meridian ∼170°W, during January-March 1996) and P15N (10°S-54°N along the meridian ∼167°W, during September-November 1994). These transects correspond to the austral summer and the boreal autumn, respectively.

https://doi.org/10.5194/egusphere-2024-4079
Preprint. Discussion started: 15 January 2025

- The zonal section transect P02T (133°E-54°W along the parallel ∼30°N, during January-February 1994). This transect corresponds to the boreal winter.
- The zonal section transects P06E (153°E-148°W along the parallel ∼31°S, during July-August 2017) and P06W (147°W-71°W along the parallel ∼32°S, during August-September 2014). These transects correspond to the austral winter.

Using the Thermodynamic Equation of SeaWater 2010 (McDougall and Barker, 2011), the Conservative Temperature (Θ), Absolute Salinity (S_A), and surface-referenced potential density (ρ_0^θ) along these transects were calculated. All these variables were interpolated vertically with a resolution of 1 m, starting at 10 m depth.

2.2.2 Argo data

Argo in situ profiles for the world ocean from January 2005 to December 2023 were used; the profiles were obtained from the Argo snapshot of June 2024 (Argo, 2024). Delayed mode profiles deemed good and probably good (quality flags 1 and 2) were selected, obtaining 2 million in situ profiles. As for the WOCE data, Θ, S_A, and ρ_0^θ were calculated using the Thermodynamic Equation of SeaWater 2010. The original vertical resolution of Argo profiles was retained to construct an observation-based global monthly MLD climatology; however, the different variables were interpolated to 10 m if there were no measurements at that depth. The spatial and temporal distribution of the Argo profiles used in this study are shown in Fig. S1 of the Supplement.

2.3 Common MLD methodologies

The performance of the energy-based MLD methodology described in section 2.1 will be contrasted with three commonly used methodologies: (i) the 0.03 kg m^{-3} and (ii) the 0.2°C thresholds of de Boyer Montégut et al. (2004), and (iii) the multi-criteria method of Holte and Talley (2009), and the recent (iv) sigmoid function fitting method by Romero et al. (2023). Hereinafter, we refer to these methodologies as B04D, B04T, HT09, and R23, respectively. To compute WB and the density and temperature thresholds, we used a reference depth of 10 m, in agreement with de Boyer Montégut et al. (2004) and Treguier et al. (2023). WB was interpolated every meter from 10 m to greater depths, and WB_z was calculated accordingly using central differences. That made it possible to compare MLD methodologies.

3 Results

The results are presented in three parts. First, we analyze a WB value that could determine the MLD in the Pacific Ocean transects during various seasons. Then, we analyze the performance of the energy-based MLD methodology in regions where common MLD methodologies do not agree on the MLD calculation. This analysis will enable us to compare the energy-based MLD methodology with others. Finally, we present the energy-based monthly climatology of the global MLD, along with the associated mixed-layer hydrography.

https://doi.org/10.5194/egusphere-2024-4079
Preprint. Discussion started: 15 January 2025

3.1 A WB value that defines the MLD

This section investigates if a single WB value can determine the MLD throughout the Pacific Ocean during various seasons. WB_z was calculated to find the depth of the structural change in WB that defines the MLD. Figure 2 shows the WB required to displace a water parcel from any depth to 10 m along each Pacific Ocean transect (upper panels) and the corresponding WB_z (lower panels) in grayscale. The location of the WOCE transects is shown in the left panels.

An upper section of the water column with relatively low WB values is shown in Fig. 2; this section increases non-linearly with greater depths. The WB and WB_z plots reflect the characteristics of vertical stratification across the Pacific Ocean during different seasons; a comprehensive discussion of the relationship between WB and stratification is beyond the scope of this study and is proposed for future research. More importantly, the WB and WB_z plots clearly show the depth of the structural change in WB, the depth at which a considerable increase in WB occurs. The question is whether this depth corresponds to a single WB value. A single WB_z value does not consistently locate the structural change in WB; it is located between the isolines 1.5 and 2.5 of WB_z. The average difference in depth between the isolines 1.5 and 2.5 of WB_z is:

- 2.4 m in transects P14S and P15N,
- 14.1 m in transect P02T, and
- 9.9 m in transects P06E and P06W.

The differences in depth between the WB_z isolines reflect the seasonal stratification characteristics in each transect: the vertical gradients of stratification and WB are strong during summer-autumn (transects P14S and P15N) and weak during winter (transects P02T, P06E, and P06W). Given the small differences in depth between the isolines 1.5 and 2.5 of WB_z, it is concluded that the depth of the structural change in WB is truly located within the depths of the 1.5-2.5 WB_z isolines.

The depth of the 1.5-2.5 WB_z interval roughly corresponds to the depth of the 10-35 WB interval (Fig. 2). To find the WB value that best locates the depth of the structural change in WB, a statistical analysis of the differences in depth between specific WB_z and WB isolines was performed. We calculated boxplots of the differences in depth between a specific WB_z isoline and various WB isolines (see Fig. S2 in the Supplement). For each WB_z isoline, we selected the WB isolines with the smallest differences in depth with respect to those in the WB_z interval, according to the following criteria: the median is lower than ± 5 m, and the difference between the third and first quartiles is lower than 10 m. Table 1 shows the results.

The 20 J m^{-3} WB isoline is the only one common to the three WB_z isolines in all transects (Table 1); the depth of such WB isoline is the one that best locates the depth of the structural change in WB. Thus, the depth of the 20 J m^{-3} WB isoline delineates an upper layer of the ocean that is well-mixed in energetic terms, which defines the MLD. This analysis shows that a single WB value can be used to define the MLD throughout the Pacific Ocean, which is a remarkable result.

We propose using inductive reasoning to define the MLD globally. Assuming that WB and WB_z behave similarly in the world ocean as in the Pacific, we suggest that the depth of the 20 J m^{-3} WB isoline can reliably define the MLD globally during all seasons. The results for the Pacific Ocean shown in the previous analyses are thus consistent with that general

https://doi.org/10.5194/egusphere-2024-4079
Preprint. Discussion started: 15 January 2025

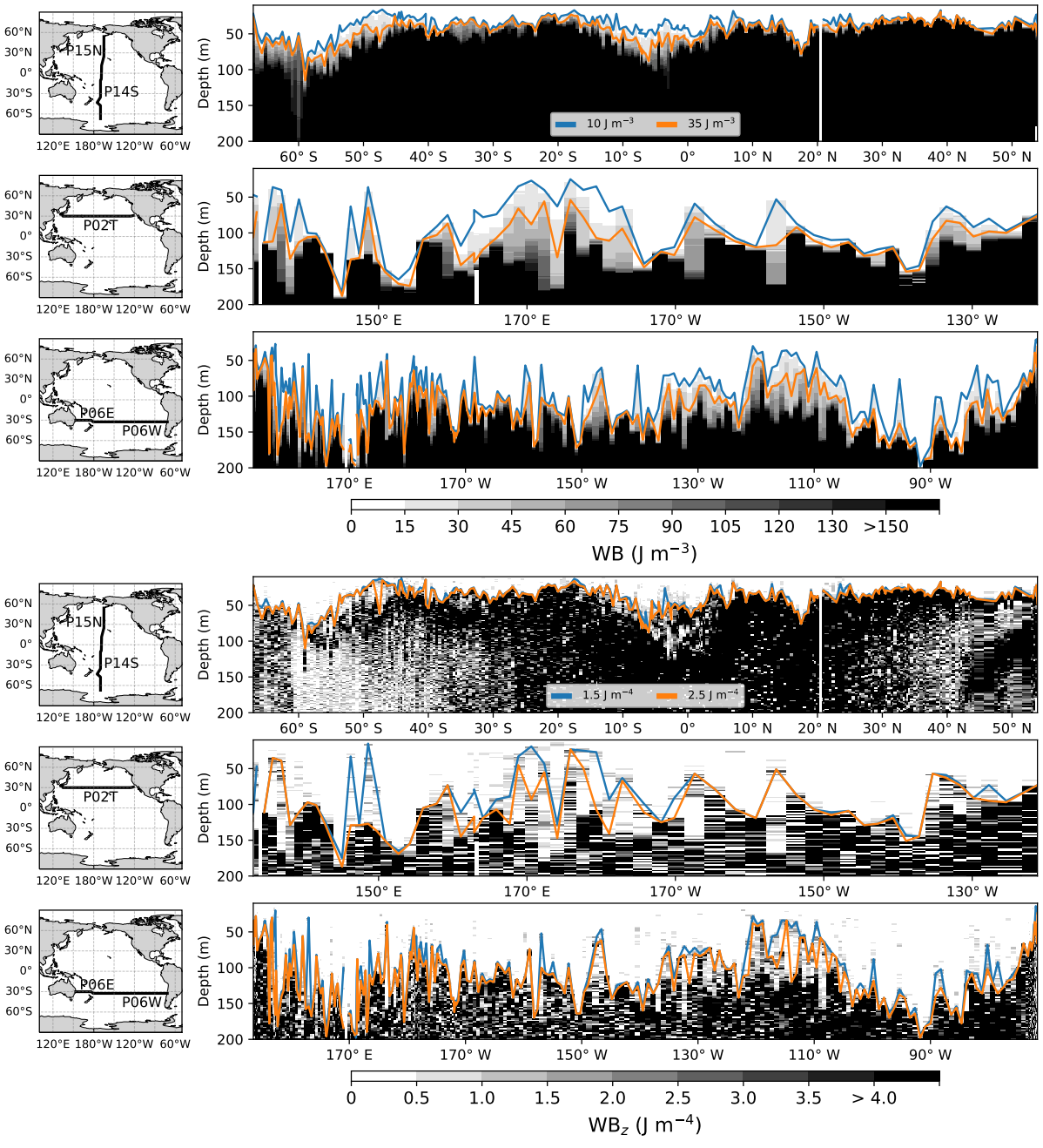

Figure 2. WB (upper panels) and WB_z (lower panels) along each Pacific Ocean transect (grayscale). For the WB plots, the 10 and 35 J m^{-3} WB isolines are shown; for the WB_z plots, the 1.5 and 2.5 J m^{-4} WB_z isolines are shown. Note that only the first 200 m of the water column are shown.

https://doi.org/10.5194/egusphere-2024-4079
Preprint. Discussion started: 15 January 2025

Table 1. Results from a statistical analysis of the differences in depth between specific WB_z and WB isolines, considering the WOCE transects. Only the WB isolines with the smallest differences in depth with respect to the 1.5, 2.0, and 2.5 J m^{-4} WB_z isolines are shown.

WBz isoline (J m^{-4})	Transects P14S and P15N	Transect P02T	Transects P06E and P06W
1.5	WB = 10, 15, 20, 25, 30, and 35 J m^{-3}	WB = 10, 15, and 20 J m^{-3}	WB = 10, 15, and 20 J m^{-3}
2	WB = 10, 15, 20, 25, 30, and 35 J m^{-3}	WB = 10, 15, 20 and 25 J m^{-3}	WB = 15, 20, 25, 30 and 35 J m^{-3}
2.5	WB = 10, 15, 20, 25, 30, and 35 J m^{-3}	WB = 20, 25, and 30 J m^{-3}	WB = 15, 20, 25, 30 and 35 J m^{-3}

assertion. The above sustains the proposal of our energy-based MLD methodology applicable to the global ocean, which will be referred to as EBM.

3.2 Performance of the energy-based MLD methodology in challenging regions

One crucial contribution of this study is the global applicability of the energy-based MLD methodology. This methodology should provide a realistic description of the MLD, consistent with the seasonal variation of local hydrography, even in challenging regions. The regions where common MLD methodologies do not agree on the MLD calculation can be considered challenging; due to the dynamics and particular hydrography of these regions, the different methodologies do not coincide when evaluating their mixing conditions. This subsection compares the performance of the energy-based methodology with that of other common methodologies in challenging regions.

3.2.1 Challenging regions for the MLD calculation

To identify the challenging regions, the global monthly MLD climatologies were first computed considering each common methodology; the Argo data were used to calculate global climatologies. The MLD was computed for each Argo profile. Within a 2°x2° grid for each month in the long-term record, the resulting MLD values were then averaged to obtain a representative value of the MLD for each cell on each given month. For each 2°x2° grid cell in a month, the absolute difference between the minimum and maximum MLD values from the four common methodologies was calculated (the MLD range). Figure 3 shows the global monthly climatology of the MLD range.

The MLD range has relatively high values ($>$ 10 m) across most of the world ocean (Fig. 3). The above reflects the subjective nature of the mixed layer definition and the resulting lack of consistency among the four common methodologies for determining the MLD. The most significant disagreements occur during winter and early spring when mixing is more active, eroding sharp density and temperature gradients in winter and creating near-surface restratification in spring. The common MLD methodologies also show low consistency in regions where salinity significantly influences density, such as polar seas, intermediate and deep-water formation regions, and barrier and compensated layers. Profiles with these characteristics present a challenge for these methodologies, which are mainly based on density and temperature thresholds, in finding the MLD. The

https://doi.org/10.5194/egusphere-2024-4079
Preprint. Discussion started: 15 January 2025

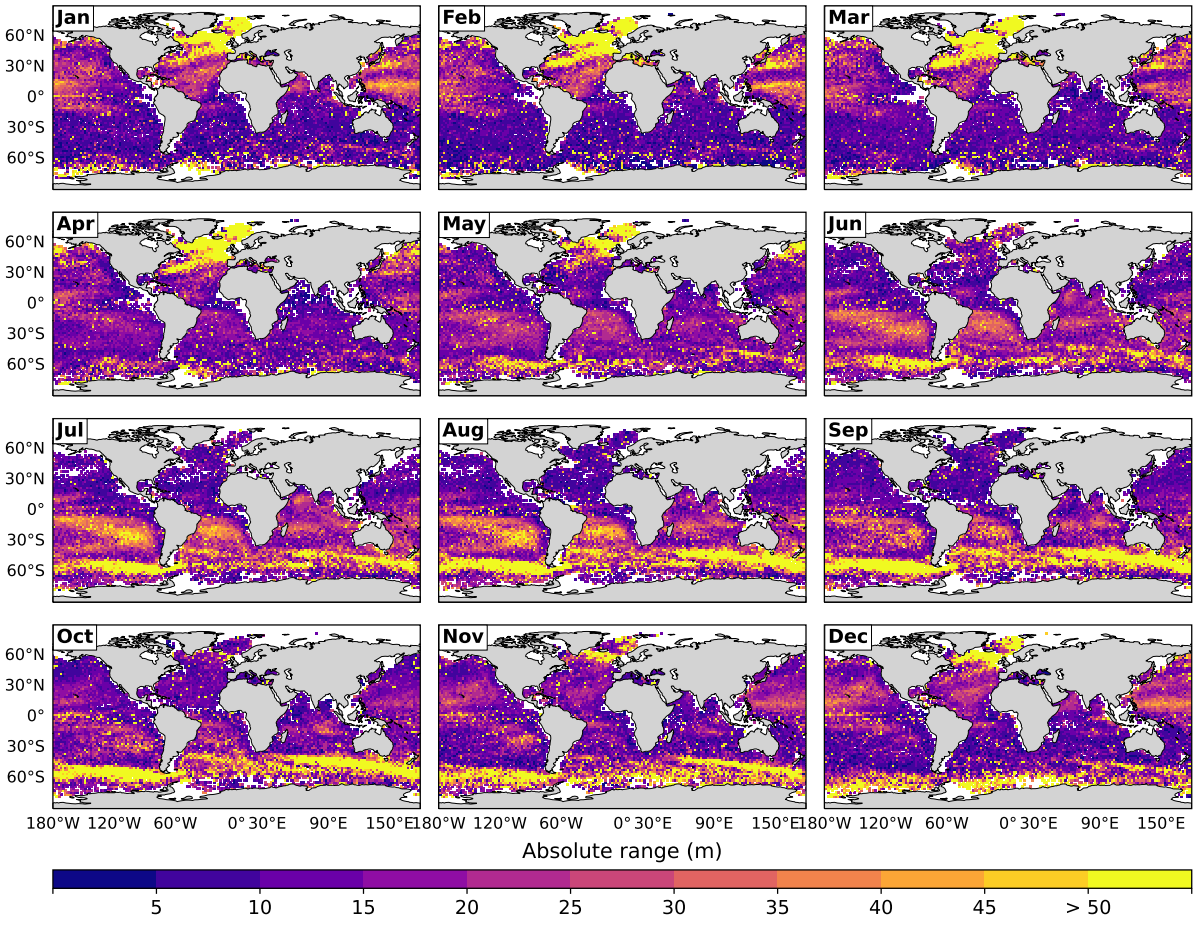

Figure 3. Global monthly climatology of the MLD range, i.e., the absolute difference between the minimum and maximum MLD values from the four common methodologies.

smallest values of the MLD range occur during summer when the pycnocline and thermocline are shallow with sharp density and temperature gradients; in these conditions, the common MLD methodologies are in agreement.

The challenging regions, thus, correspond to the regions with high MLD range values. The threshold value associated with those high MLD range values was determined using a statistical outlier detection method. A probability distribution was constructed from the monthly climatology of the MLD range, and its upper limit (or maximum non-atypical) was calculated according to $Q_3 + [1.5(Q_3 - Q_1)]$, where Q_1 and Q_3 are the first and third quartiles, respectively. The resulting upper limit value was 50 m (the 91st percentile of the probability distribution); thus, the challenging regions correspond to the regions with MLD range values higher than 50 m. Three regions resulted (regions colored yellow on the map in Fig. 3): (i) the Southern Ocean (∼65-40°S) during austral winter (July, August, September) and part of spring (October and November), (ii) the North

https://doi.org/10.5194/egusphere-2024-4079
Preprint. Discussion started: 15 January 2025

Atlantic ($> 30°$N) during boreal winter (January, February, March) and early spring (April), and (iii) the subtropical eastern Pacific ($\sim$0-30°S) during austral winter (July and August).

3.2.2 MLD methodologies intercomparison

The performance of the energy-based methodology was compared with that of the common methodologies by analyzing random profiles in the three identified challenging regions. Figure 4 shows the vertical profiles of WB, σ_0, Θ, and S_A and the corresponding MLD calculated with each methodology in five locations for each challenging region. For each profile shown in Fig. 4, Tables S1-S3 in the Supplement show the MLD and the differences in σ_0, Θ, and WB from the reference depth of 10 m to the MLD calculated with each methodology.

In the challenging regions, there is no consensus on the MLD calculation; in principle, no single methodology should be preferred over the others. The following is observed regarding the ability of each methodology to identify a relatively homogeneous upper ocean layer in the challenging regions (Fig. 4). All the methodologies approximately coincide in the MLD calculation for ideal profiles, that is, for hydrographic profiles with a clear homogeneous upper section and sharp density and temperature gradients below it, without temperature inversions. For profiles with increasing density and decreasing temperature from the near-surface, all the methodologies give very shallow MLD values, which do not necessarily coincide. The most significant disparity in the MLD values is obtained for profiles with a quasi-homogeneous upper section and smooth gradients below it; these profiles are ubiquitous in the challenging regions and are primarily responsible for the significant disagreement on the MLD calculation. In some cases, some common methodologies fail to provide a MLD value.

The common methodologies provide an ensemble of the possible extent of the mixed layer, in which the smallest and largest values of the MLD account for the uncertainty in calculating it. In this ensemble approach, the energy-based methodology gives MLD values close to the shallowest or between the extreme ones calculated with the common methodologies (Fig. 4). Furthermore, due to its construction, the energy-based methodology performs without failure under every ocean condition. In contrast, the common methodologies are prone to fail when analyzing hydrographic profiles differing from the ideal ones. Therefore, it is concluded that the energy-based methodology is robust under different ocean conditions and provides realistic estimates of the MLD in challenging regions. Next, we provide some specificities concerning the performance of the MLD methodologies for each challenging region.

The profiles in the Southern Ocean (Figs. 4a-e) exhibit notorious temperature inversions, which cause the homogeneous density layer to not coincide with the homogeneous temperature layer. Generally, the homogeneous temperature layer is deeper than the homogeneous density layer; therefore, B04T generally identifies inhomogeneous upper sections in every hydrographic variable. For the profiles in Figs. 4a-b, all the methodologies perform well according to their criteria and give similar MLD values. The profiles in Figs. 4c-d have the highest disparity in the MLD calculation; compared to the common methodologies, EBM better identifies the relatively homogeneous upper ocean layer by providing the shallowest MLD values. For the profile in Fig. 4e, R23 performs best in identifying the MLD; however, EBM identifies the upper homogeneous layer associated with near-surface restratification.

https://doi.org/10.5194/egusphere-2024-4079
Preprint. Discussion started: 15 January 2025

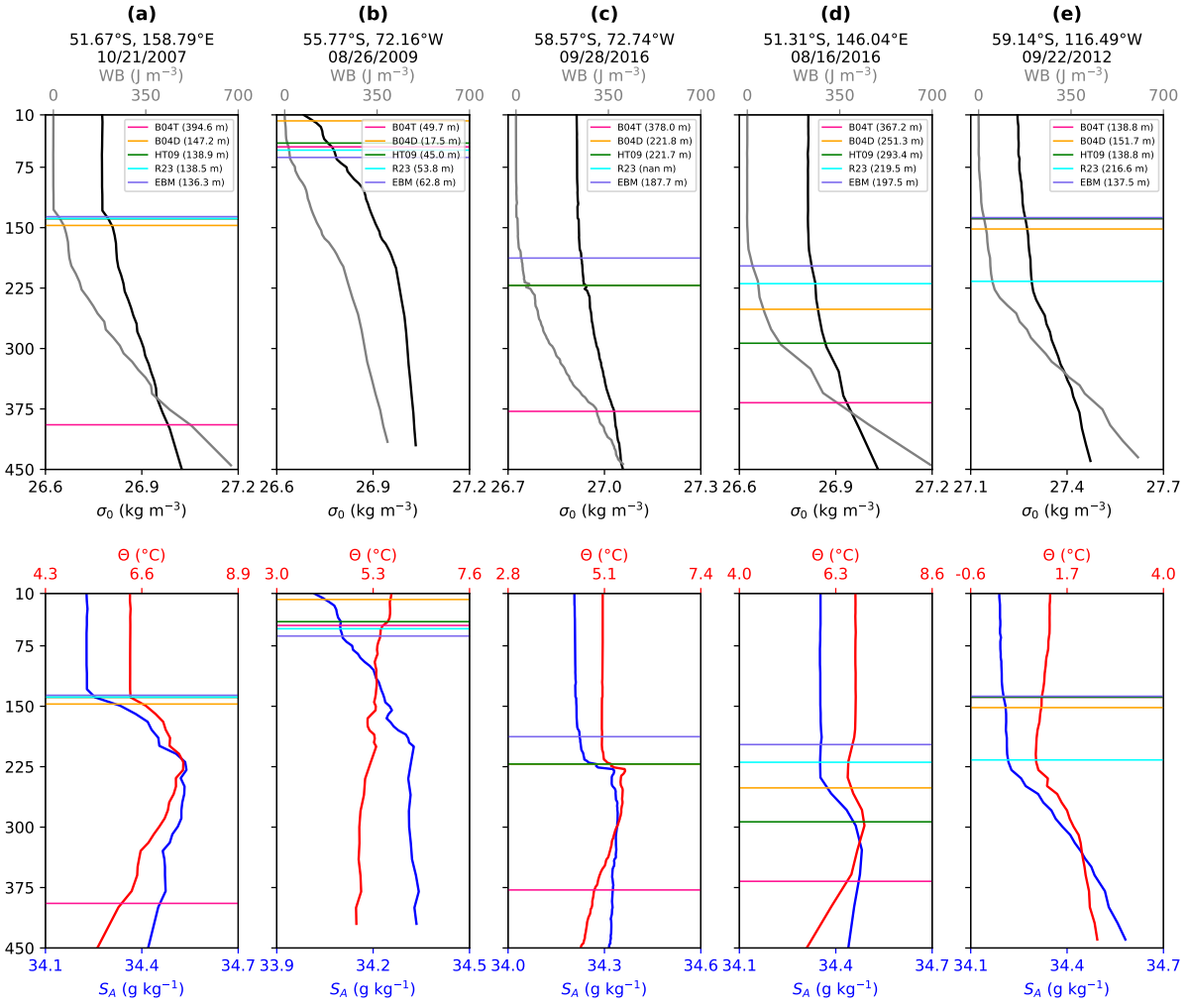

Figure 4. Part one. Random profiles in the Southern Ocean. Vertical profiles of WB, σ_0, Θ, and S_A and the corresponding MLD calculated with each methodology are shown.

The profiles in the North Atlantic (Figs. 4f-j) exhibit a high disparity in the MLD calculation, except for the profile in Fig. 4i, in which all the methodologies provide shallow and similar MLD values. All the methodologies perform well according to their criteria for the profiles in Figs. 4f and 4h, and no methodology is preferred over any other. Temperature inversions also occur in this region (profiles in Figs. 4i-j); B04T fails to estimate the MLD, whereas EBM performs very well in identifying the relatively homogeneous upper ocean layer. The quasi-homogeneous profile in Fig. 4g represents a real challenge for calculating the MLD; B04D and R23 fail, whereas EBM provides a value between HT09 and B04T.

The hydrography in the subtropical eastern Pacific (Figs. 4k-o) has the largest variations compared to the other challenging regions; consequently, the MLD is the shallowest. In that region, profiles with a quasi-homogeneous upper section and smooth

https://doi.org/10.5194/egusphere-2024-4079
Preprint. Discussion started: 15 January 2025

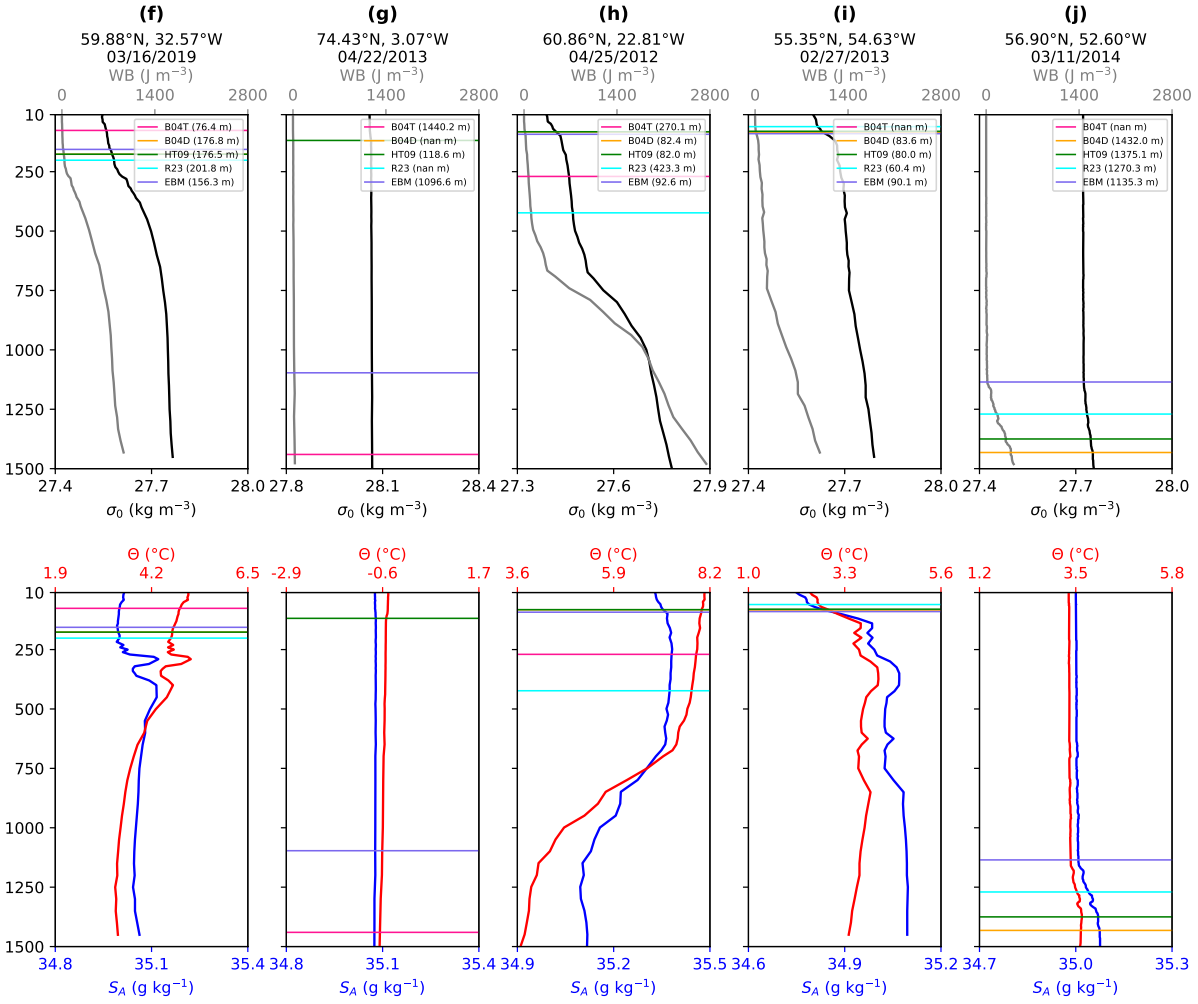

Figure 4. Part two. Random profiles in the North Atlantic.

gradients below it predominate, besides profiles with near-surface restratification and slight temperature inversions. The calculated MLD is very dissimilar among all the methodologies, except for the profile in Fig. 4l, in which all the methodologies provide similar values. Again, all the methodologies perform well according to their criteria, and no methodology is preferred over any other. EBM is supported because it provides MLD values between the extremes calculated with the common methodologies. In an ensemble approach, such values represent realistic estimates of the MLD. Generally, B04D and HT09 provide the smallest MLD values, whereas B04T and R23 provide the largest MLD values.

https://doi.org/10.5194/egusphere-2024-4079
Preprint. Discussion started: 15 January 2025

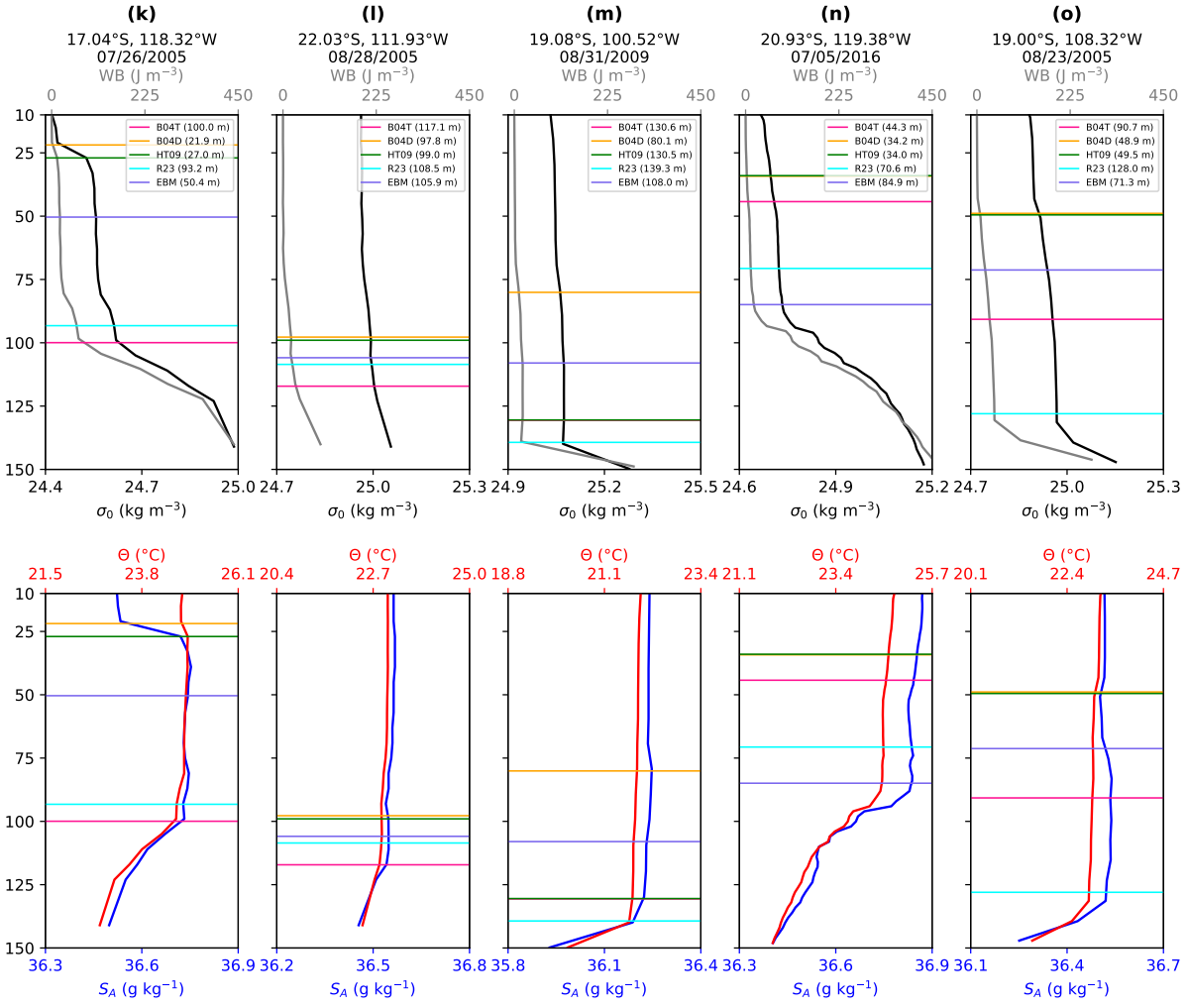

Figure 4. Part three. Random profiles in the subtropical eastern Pacific.

3.3 Global monthly MLD climatology and mixed layer hydrography

The global monthly MLD climatology calculated with EBM is shown in Fig. 5. The MLD is highly heterogeneous in space. The tropical oceans have relatively shallow mixed layers throughout the year, with moderate seasonal changes; the MLD varies in a few tens of meters range. Semiannual cycles can be discerned in the region of barrier layer formation, approximately located in $[15°\mathrm{S}, 15°\mathrm{N}] \times [150°\mathrm{E}, 150°\mathrm{W}]$, and in the northern Indian Ocean, mainly in the Arabian Sea. In contrast to the tropical oceans, the regions from midlatitudes to high latitudes have deeper mixed layers with strong seasonal behavior, with the MLD ranging from several tens of meters during summer and early autumn to a few hundred meters during winter and early spring. The largest MLD values occur during wintertime in deep and intermediate water formation regions and polar seas in the North

https://doi.org/10.5194/egusphere-2024-4079
Preprint. Discussion started: 15 January 2025

Atlantic (south of Iceland and the Labrador, Greenland, Iceland, and Norway Seas) and the southern Pacific and Indian Oceans between 65°S and 45°S. The MLD can reach depths of up to 650 m in the south of Iceland and the Labrador Sea, 750 m in the Greenland, Iceland, and Norway Seas, and 600 m in the southern Pacific and Indian Oceans. The MLD values in the northern Pacific are asymmetric during wintertime; they are larger in the northwest than in the northeast.

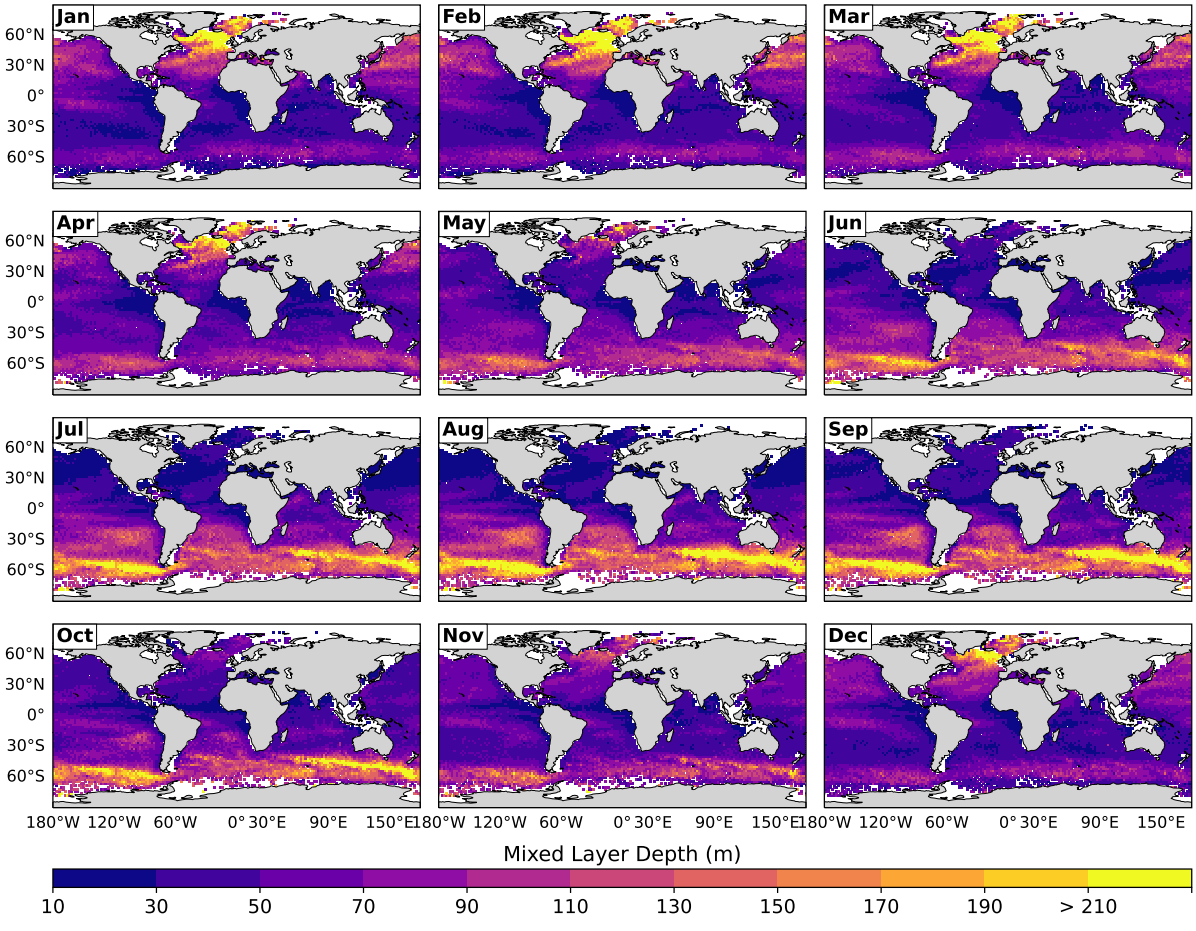

Figure 5. Energy-based global monthly MLD climatology, calculated with the Argo data.

A map of the energy-based MLD in the Southern Ocean is shown in Fig. 6; a typical month for each austral season is shown: February (summer), May (autumn), August (winter), and November (spring). In agreement with the expected physical behavior, the MLD exhibits clear seasonality, shallow during summer and deep during winter. During each season, the mixed layer is shallow in the continental shelves, deepens in the Antarctic Circumpolar Current region, and becomes shallower towards the north of the Antarctic Circumpolar Current. The largest MLD values are located south of the Pacific and Indian Oceans, where they can reach 600 m depth. The largest MLD values are not located between the same latitudes; they are located between 60°S-50°S in the Pacific, between 50°S-40°S in the Indian Ocean, and between 60°S-50°S in the Atlantic Ocean.

https://doi.org/10.5194/egusphere-2024-4079
Preprint. Discussion started: 15 January 2025

To extend our understanding of the Southern Ocean, the histograms (expressed in densities) of the monthly MLD for this region are also shown in Fig. 6. The histograms are not symmetrical and exhibit an appreciable bimodal distribution during summer, which tends to diminish over time until it disappears during winter. The MLD is concentrated on values of around 30-80 m during summer and around 110-150 m during winter; such behavior is accompanied by MLD variances increasing from about 300 m during summer to 3000 m during winter, in agreement with Johnson and Lyman (2022). The MLD distribution has a persistent positive skewness throughout the year, with the shortest tail during austral summer (skewness=0.42) and the largest during austral winter (skewness=1.33). This behavior does not agree with Johnson and Lyman (2022), who found that the MLD skewness changes from negative in May to positive in November using the HT09 methodology.

The previous analyses showed that the energy-based methodology provides realistic estimates of the MLD, consistent with the density stratification intensity in all world regions, demonstrating the good performance of the methodology and its global applicability during all seasons. The energy-based methodology determines a mixed layer homogeneous in buoyancy energy, which does not always coincide with a homogeneous density or temperature layer. Figures 7 and 8 show a monthly climatology of potential density differences and conservative temperature differences from the reference depth (10 m) to the energy-based MLD. These figures also show histograms (expressed in densities) of such density and temperature differences considering all the months; thus, they represent the conjoint distribution in space and time of the density and temperature differences.

In general, the potential density differences (Fig. 7) have a behavior opposite to that of the MLD (Fig. 5), mainly due to the density stratification characteristics. The stronger the density stratification, the smaller the MLD and the larger the density differences; the weaker the density stratification, the larger the MLD and the smaller the density differences. The density differences are highly heterogeneous in space, larger in the northern hemisphere than in the southern hemisphere. The tropical oceans have large differences with a strong seasonal variation. As for the MLD, semiannual cycles can be discerned in the region of barrier layer formation, approximately located in $[15°\text{S}, 15°\text{N}] \times [150°\text{E}, 150°\text{W}]$, and in the northern Indian Ocean. The mid-to-high latitudes oceans exhibit strong seasonal behavior, with small density differences during wintertime and large during summertime. The Southern Ocean (65°S-40°S) exhibits small density differences of around 0.03 kg m^{-3} almost throughout the year despite having a strong MLD seasonal variation; the density differences slightly increase during winter. The corresponding histogram shows that 75% of the world ocean has density differences of up to 0.11 kg m^{-3} throughout the year. The energy-based methodology determines a homogeneous mixed layer in buoyancy energy and a quasi-homogeneous density layer for most of the world ocean.

As expected, the monthly climatology of conservative temperature differences (Fig. 8) has characteristics that are opposite to those of the MLD climatology (Fig. 5). The stronger the temperature stratification, the smaller the MLD and the larger the temperature differences; the weaker the temperature stratification, the larger the MLD and the smaller the temperature differences. The temperature differences are highly heterogeneous in space. The tropical oceans have the smallest differences, with a strong seasonal variation in the eastern Pacific Ocean and a semiannual cycle in the northern Indian Ocean. The mid-to-high latitudes oceans exhibit strong seasonal behavior, with small temperature differences during wintertime and large during summertime. The temperature differences are larger in the northern hemisphere than in the southern hemisphere. The Southern Ocean (65-40°S) exhibits seasonal temperature differences from around 0.1°C during winter to more than 0.4°C

https://doi.org/10.5194/egusphere-2024-4079
Preprint. Discussion started: 15 January 2025

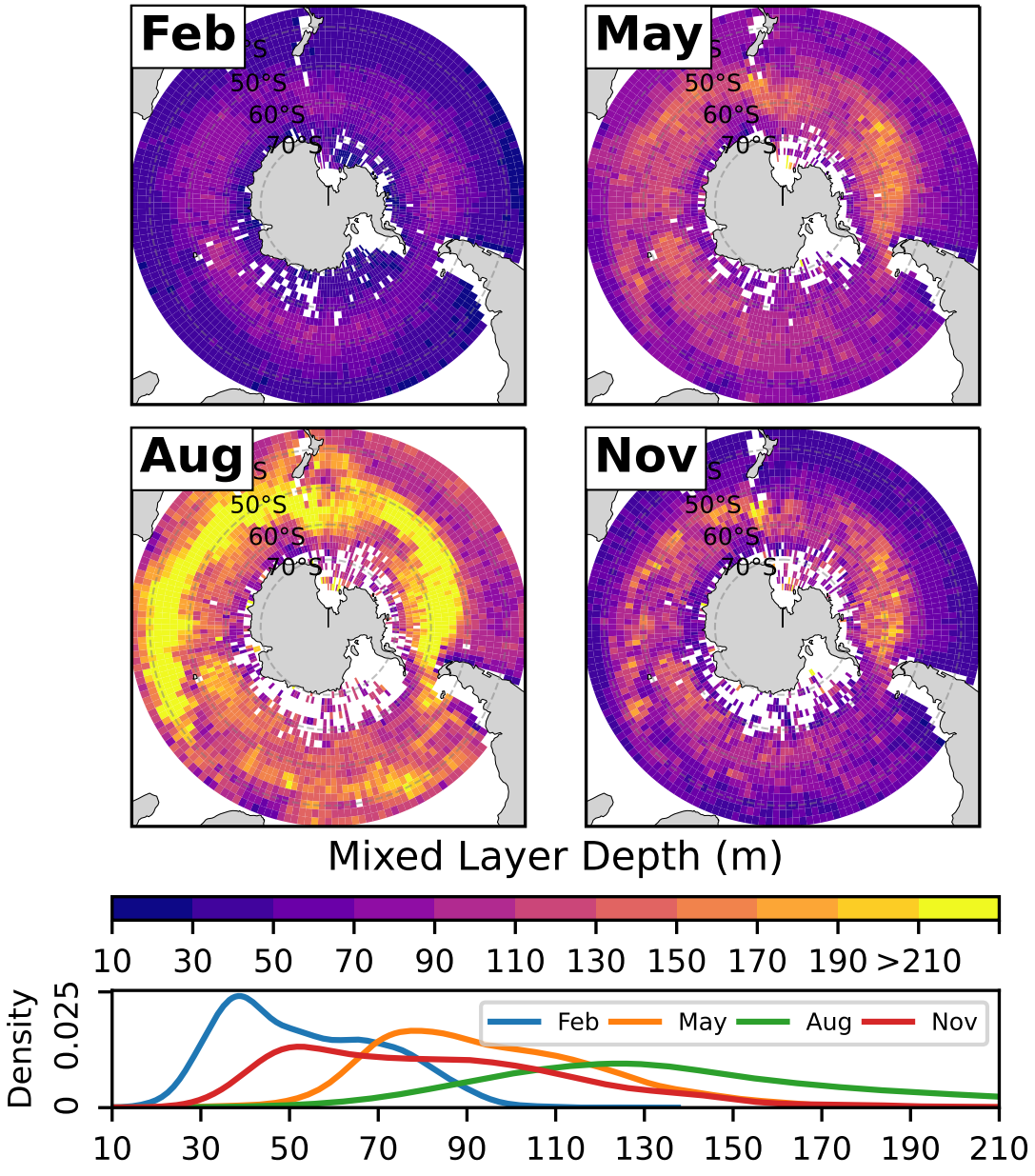

Figure 6. Upper panels: energy-based MLD in the Southern Ocean in a typical climatological month for each austral season: February (summer), May (autumn), August (winter), and November (spring). Lower panel: histograms (expressed in densities) of the corresponding MLD during each typical month.

https://doi.org/10.5194/egusphere-2024-4079
Preprint. Discussion started: 15 January 2025

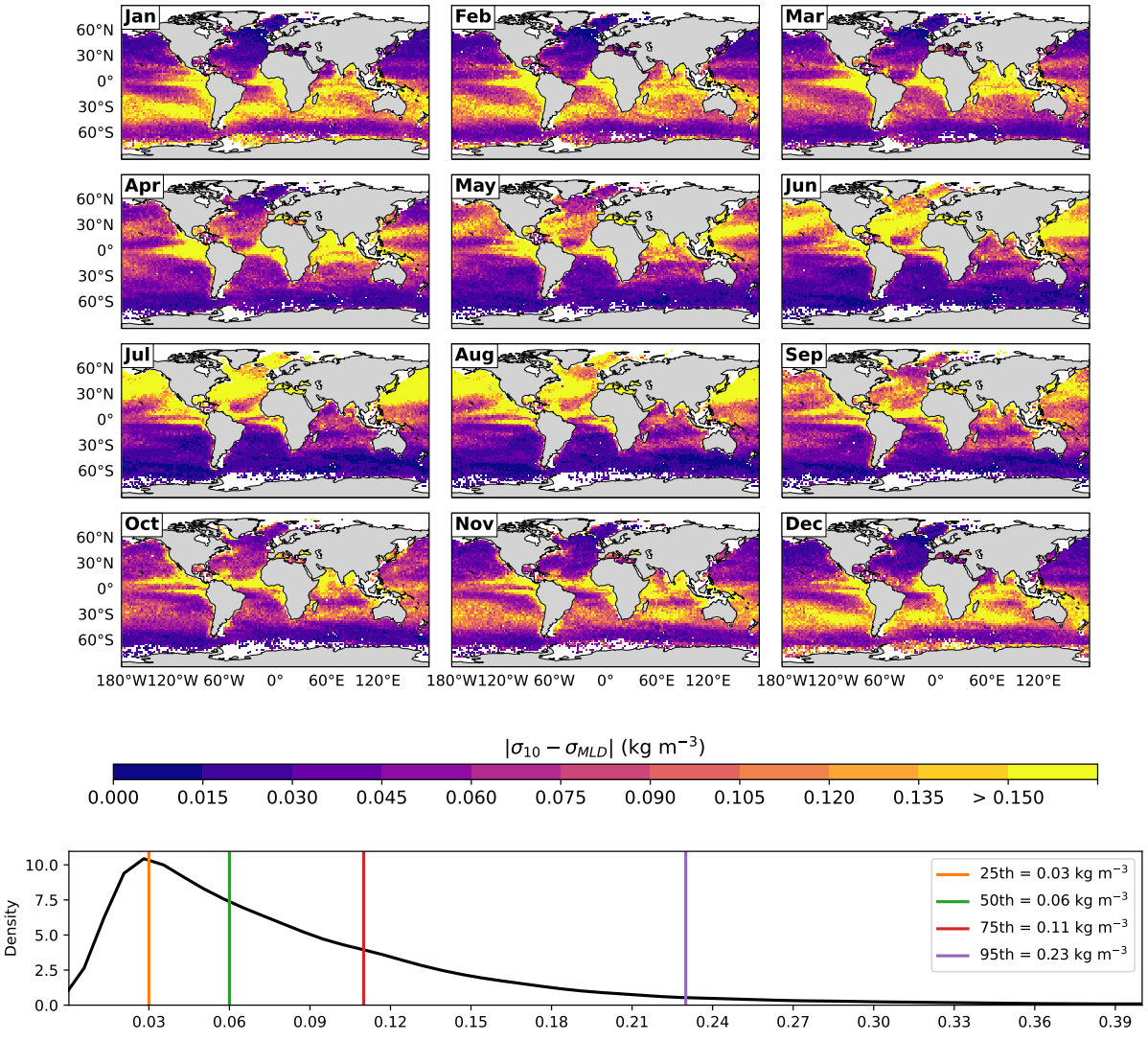

Figure 7. Upper panel: global monthly climatology of absolute differences in potential density from the reference depth of 10 m to the energy-based MLD. The maximum density difference is 1.43 kg m^{-3}. Lower panel: the histogram (expressed in densities) of the conjoint distribution in space and time of the density differences. The values of the histogram at various percentiles are also shown.

during summer, consistent with its strong MLD seasonal variation. The corresponding histogram shows that 95% of the world ocean has temperature differences of up to 0.74°C throughout the year. Again, the homogeneous mixed layer in buoyancy energy approximately coincides with a quasi-homogeneous temperature layer for most of the world ocean.

https://doi.org/10.5194/egusphere-2024-4079
Preprint. Discussion started: 15 January 2025

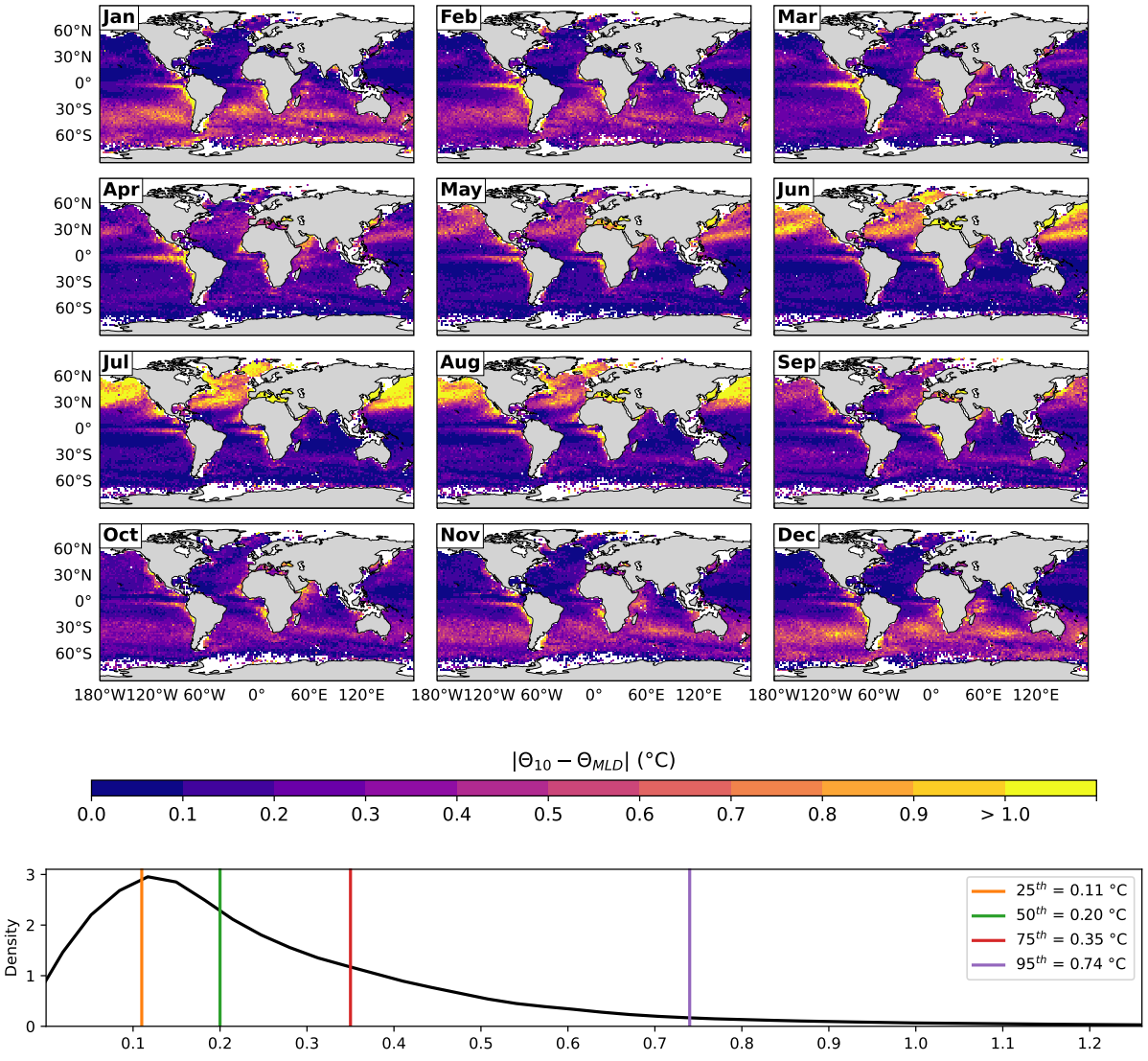

Figure 8. Upper panel: global monthly climatology of absolute differences in conservative temperature from the reference depth of 10 m to the energy-based MLD. The maximum temperature difference is 6.33°C. Lower panel: the histogram (expressed in densities) of the conjoint distribution in space and time of the temperature differences. The values of the histogram at various percentiles are also shown.

4 Discussion

In this study, we developed a new methodology constructed from physical principles and energy considerations for calculating the MLD. Our study advances the development of energy-based methodologies to define the MLD, adding to that of Reichl et al. (2022). The most important characteristic of our energy-based methodology is that it provides realistic estimates of the

https://doi.org/10.5194/egusphere-2024-4079
Preprint. Discussion started: 15 January 2025

MLD in all world regions under different ocean conditions using a consistent criterion in space and time, that is, a criterion that does not vary in space or time depending on the hydrography of the study region. The procedure for calculating the MLD using the energy-based MLD methodology is as follows. From a vertical profile of surface-referenced potential density, calculate the WB required to displace a water parcel from all depths to 10 m and find the depth of the 20 J m^{-3} WB isoline, which defines the MLD. The energy-based methodology performs well during periods and in regions where the common methodologies show low consistency in the MLD calculation (in the so-called challenging regions). The methodology is, therefore, accurate, robust, and of global applicability. It can be the base methodology for performing MLD model intercomparison studies, as in the OMIP and CMIP projects (Griffies et al., 2016; Treguier et al., 2023). It is also easy to implement numerically.

The energy-based methodology identifies the upper section of the ocean, well-mixed in energetic terms, that can be considered in contact with the atmosphere and thus be referred to as the mixed layer. The methodology uses the work done by the buoyancy force and the depth of its structural change to define the MLD. From the physical principles of the ocean boundary layer mixing, Reichl et al. (2022) demonstrated that diagnosing the MLD from density stratification establishes a connection between the turbulent boundary layer and the mixed layer. They demonstrated that the mixed layer can be defined through the potential energy of the water column and advocated using an energy threshold to define the MLD. There is a correspondence between our methodology and that of Reichl et al. (2022), suggesting that our energy-based methodology is consistent with the turbulence approach of the mixed layer formation (D'Asaro, 2014; Sutherland et al., 2014; Franks, 2014; Sallée et al., 2021). The mixed layer is thus determined by energy processes instead of density, temperature, or salinity thresholds, which vary in space and time according to the hydrography of the study region (Griffies et al., 2016; Treguier et al., 2023).

One of our most significant contributions is the finding that the 20 J m^{-3} WB isoline delimitates an upper section of the ocean that is well-mixed in energetic terms, defining the MLD globally during all months. This finding contrasts with Reichl et al. (2022), who did not provide specific energy values to define the MLD across the world ocean during all seasons. They found that a spatially and temporally variable energy threshold should be used to reproduce, to some extent, MLDs similar to those obtained with the HT09 methodology. However, since the common methodologies are non-energy-based, trying to match the performance of energy-based methodologies to that of non-energy-based ones may not be meaningful. To what extent are the common methodologies energy-consistent in space and time? To address this question, we considered the global MLD monthly climatology obtained with each methodology and calculated the WB value at the corresponding MLD (see Figs. S3-S6 in the Supplement). As an example, Fig. 9 shows the WB value at the MLD on a global meridional transect along 170°W during wintertime and summertime.

The 20 J m^{-3} WB isoline of the EBM methodology can be used to analyze the energy consistency of the common MLD methodologies shown in Fig. 9. The common methodologies are not energy-consistent: no unique WB value exists at the MLD. The WB variations are region- and season-dependent and differ among the methodologies. B04T has the largest WB values, followed by HT09; the largest WB values occur during winter in the polar and tropical regions and summer in the tropical regions. B04T and HT09 have WB values larger than 20 J m^{-3} throughout the transect during winter; during summer, they have WB values close to 20 J m^{-3} south of 20°S, WB values close to 20 J m^{-3} between 20°S-20°N, and WB values smaller 20 J m^{-3} north of 20°N. R23 has WB values close to 20 J m^{-3} between 55°S-40°N (where the methodology has its best fit)

https://doi.org/10.5194/egusphere-2024-4079
Preprint. Discussion started: 15 January 2025

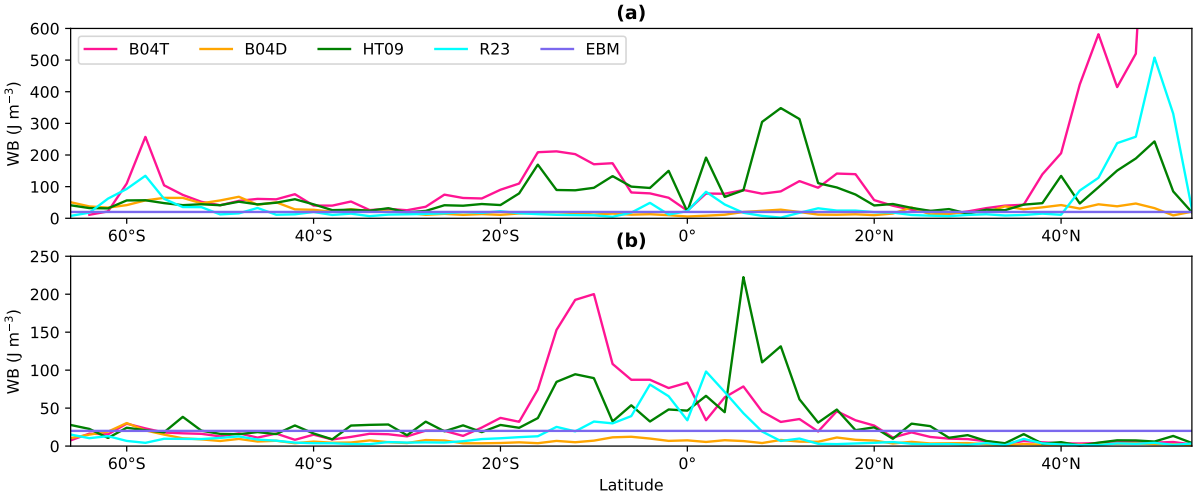

Figure 9. The WB value at the MLD for each methodology on a global meridional transect along 170°W during (a) wintertime (August in the southern hemisphere and February in the northern hemisphere) and (b) summertime (February in the southern hemisphere and August in the northern hemisphere). The global MLD monthly climatology obtained with each methodology was used for the calculation.

during winter; beyond that, the WB values are larger than 20 J m^{-3}. During summer, R23 has WB values smaller than 20 J m^{-3} along most of the transect, except near the equator, where it has WB values larger than 20 J m^{-3}. B04D shows the greatest concordance with EBM, as both are built from the density. During winter, B04D has WB values close to 20 J m^{-3} between 40°S-40°N, which increase beyond those latitudes; during summer, it has WB values smaller than 20 J m^{-3} along most of the transect.

If a MLD methodology is not energy-consistent, the homogeneity of the mixed layer in energetic terms is not equal throughout space and time; large WB values are associated with high-energy stratified layers and vice versa. The above suggests that the methodologies in which the WB at the MLD varies a lot in space and time are not expected to calculate the MLD accurately, as we showed. The common MLD methodologies analyzed in this study are non-energy-based and consequently not energy-consistent.

Common and energy-based methodologies use a threshold to define the MLD. However, the nature of their thresholds is substantially different: common thresholds only consider the difference in values of some hydrographic variable between two depths, while energy thresholds consider the cumulative effects of those differences along the vertical. As shown in this study and by Reichl et al. (2022), mixing resistance depends on the differences in density and the physical distance between two depths. While the buoyancy force is directly proportional to the difference in density between two depths, the associated work is not. That means that the difference in density between two given depths cannot be used as a proxy for the energy required to homogenize the ocean's upper layer. Similarly, density-derived measures of the local stability or homogeneity of the water column, such as the buoyancy frequency, also cannot be used as proxies for the energy required to homogenize the water column if they do not consider the cumulative effect of the buoyancy force along a water column section. Therefore, the

https://doi.org/10.5194/egusphere-2024-4079
Preprint. Discussion started: 15 January 2025

density threshold, density gradient, and buoyancy frequency criteria may not be sufficient to calculate the MLD, as done in previous research (Lukas and Lindstrom, 1991; Large et al., 1997; de Boyer Montégut et al., 2004; Lorbacher et al., 2006; Dong et al., 2008; Holte and Talley, 2009; Chu and Fan, 2011; Carvalho et al., 2017).

The definition of the mixed layer as the ocean's surface layer whose properties (density, temperature, salinity, and other tracers) are relatively homogeneous in the vertical is challenging to achieve when considering constant increases in density or constant decreases in temperature from the corresponding values of these variables at the reference depth. Since the coefficients of the equation of state of seawater vary with pressure, temperature, and salinity, a given density change does not correspond to a unique temperature change, and vice versa. In order to determine a homogeneous mixed layer from density or temperature thresholds, the thresholds should vary according to the hydrography of the study region; moreover, the implementation of spatially variable thresholds in a set of models and observations would be complex and daunting (Griffies et al., 2016; Treguier et al., 2023). Our results showed that constant density or temperature thresholds do not correspond to constant increases in WB across the world ocean. The above supports the definition of the mixed layer as the ocean's upper layer quasi-homogeneous in buoyancy energy, even if that leads to spatially variable increments in density and decrements in temperature. According to Levitus (1982) and Kara et al. (2000), variations of up to 0.125 kg m^{-3} in density and up to 0.8°C in temperature can be considered typical in a well-mixed layer. Although our methodology does not seek to determine mixed layers homogeneous in density or temperature, the energy-based mixed layer is not far from such quasi-homogeneity: 75% of the world ocean has density differences of up to 0.11 kg m^{-3}, and 95% of the world ocean has temperature differences of up to 0.74°C throughout the year.

The energy-based methodology is sensitive to the choice of the reference depth, mainly in regions with very thin mixed layers and during winter and early spring when mixing is more active, eroding sharp density and temperature gradients in winter and creating near-surface restratification in spring (the so-called challenging regions). The above is not a limitation of our methodology since it is based on the structural change in WB; it still can be used to find the exact WB isoline that defines the MLD. For those regions and during those periods, the reference depth has to be adapted to be consistent with the local dynamics; then, the depth of the structural change in WB can be found using its vertical gradient or a specific ad-hoc method and thus locate the MLD. Furthermore, we explored the influence of the vertical resolution of the density profiles on the MLD calculation. We found that as long as the vertical characteristics of the density are correctly resolved and sampled, the estimated MLD will be accurate to the order of the vertical resolution. This adaptability provides flexibility in applying the methodology in specific regions and under different ocean conditions.

This study analyzed the MLD on long spatial and temporal scales: spatial scales larger than mesoscale and timescales larger than diurnal cycles. Active mixing and high-frequency MLD variability, mainly driven by synoptic atmospheric forcing, ocean eddies, and fronts (Brainerd and Gregg, 1995; Whitt et al., 2019), were not addressed. To explore the above processes, the surface turbulent boundary layer is a more relevant measure (Reichl et al., 2022). In computing monthly MLD values from daily values, the sub-monthly variability was omitted, potentially underestimating the MLD compared to the corresponding daily MLD values, as shown by Toyoda et al. (2017). A thorough analysis of regional differences between the monthly and daily MLD values is out of the scope of this study and is proposed for future research. The MLD analysis in the Southern

https://doi.org/10.5194/egusphere-2024-4079
Preprint. Discussion started: 15 January 2025

Ocean revealed additional differences between the energy-based and non-energy-based methodologies regarding the skewness of the MLD distribution and its persistence. Further analyses of those differences are beyond the scope of this study and are also proposed for future research. Finally, future research proposes quantifying the runtime to estimate the MLD in on-the-fly or offline computations, considering different MLD methodologies.

5 Conclusions

Recent research has proposed energy-based methodologies as the best option to calculate the MLD, as they can provide accurate estimates while maintaining the calculations without the unnecessary complexities of the turbulent mixing theory. We contribute to the development of energy-based methodologies to define the MLD. Based on energy considerations, our proposed MLD methodology is globally applicable and produces realistic estimates of the MLD. We found that a unique energy equipotential can define the MLD across the world ocean throughout the year. The mixed layer, determined by energy processes, is also quasi-homogeneous in density and temperature in most of the global ocean during most of the year.

A practical contribution of our work is an observation-based global MLD climatology, useful for seasonal to climate time scale studies from regional to large spatial scales. This climatology can also be used as a reference to validate Oceanic General Circulation Model solutions and perform MLD model intercomparison studies. Currently, we are working on investigating the potential of this new MLD methodology to better interpret various dynamic (e.g., vertical exchanges within the ocean and between the ocean and the atmosphere), thermodynamic (e.g., upper ocean heat content), and ecological (e.g., chlorophyll-a content and phytoplankton dynamics) processes at regional and global scales.

Code availability. The methodology presented in this study is licensed under a GNU General Public License v3.0. The source code is available at https://doi.org/10.5281/zenodo.14531829. The latest package version is v1.0.1.

Author contributions. EM conceived and designed the study, developed the methodology, wrote the scripts, interpreted the results, wrote and revised the manuscript, and acquired funding. ER designed the study, wrote the scripts, analyzed the data, interpreted the results, created the figures, and wrote and revised the manuscript. KR-M designed the study, developed the methodology, wrote the scripts, interpreted the results, and wrote and revised the manuscript. LT-F designed the study, interpreted the results, and revised the manuscript. All authors contributed substantially to this work and approved it for publication.

Competing interests. The authors declare that they have no conflict of interest.

https://doi.org/10.5194/egusphere-2024-4079
Preprint. Discussion started: 15 January 2025

Acknowledgements. The authors acknowledge León Felipe Álvarez-Sánchez for his support in preparing the source code of the methodology for the GitHub platform.

https://doi.org/10.5194/egusphere-2024-4079
Preprint. Discussion started: 15 January 2025

References

Argo: Argo float data and metadata from Global Data Assembly Centre (Argo GDAC), https://doi.org/10.17882/42182, 2024.

Bopp, L., Lévy, M., Resplandy, L., and Sallée, J. B.: Pathways of anthropogenic carbon subduction in the global ocean, Geophysical Research Letters, 42, 6416–6423, https://doi.org/10.1002/2015GL065073, 2015.

Bouman, H. A., Jackson, T., Sathyendranath, S., and Platt, T.: Vertical structure in chlorophyll profiles: influence on primary production in the Arctic Ocean, Philosophical Transactions of the Royal Society A: Mathematical, Physical and Engineering Sciences, 378, 20190351, https://doi.org/10.1098/rsta.2019.0351, 2020.

Brainerd, K. E. and Gregg, M. C.: Surface mixed and mixing layer depths, Deep Sea Research Part I: Oceanographic Research Papers, 42, 1521–1543, https://doi.org/10.1016/0967-0637(95)00068-H, 1995.

Briseño Avena, C., Prairie, J. C., Franks, P. J. S., and Jaffe, J. S.: Comparing Vertical Distributions of Chl-a Fluorescence, Marine Snow, and Taxon-Specific Zooplankton in Relation to Density Using High-Resolution Optical Measurements, Frontiers in Marine Science, 7, 602, https://doi.org/10.3389/fmars.2020.00602, 2020.

Carvalho, F., Kohut, J., Oliver, M. J., and Schofield, O.: Defining the ecologically relevant mixed-layer depth for Antarctica's coastal seas, Geophysical Research Letters, 44, 338–345, https://doi.org/10.1002/2016GL071205, 2017.

Chu, P. C. and Fan, C.: Maximum angle method for determining mixed layer depth from seaglider data, Journal of Oceanography, 67, 219–230, https://doi.org/10.1007/s10872-011-0019-2, 2011.

D'Asaro, E. A.: Turbulence in the Upper-Ocean Mixed Layer, Annual Review of Marine Science, 6, 101–115, https://doi.org/10.1146/annurev-marine-010213-135138, 2014.

de Boyer Montégut, C., Madec, G., Fischer, A. S., Lazar, A., and Iudicone, D.: Mixed layer depth over the global ocean: An examination of profile data and a profile-based climatology, Journal of Geophysical Research: Oceans, 109, 2004JC002378, https://doi.org/10.1029/2004JC002378, 2004.

Deser, C., Alexander, M. A., Xie, S.-P., and Phillips, A. S.: Sea Surface Temperature Variability: Patterns and Mechanisms, Annual Review of Marine Science, 2, 115–143, https://doi.org/10.1146/annurev-marine-120408-151453, 2010.

Dong, S., Sprintall, J., Gille, S. T., and Talley, L.: Southern Ocean mixed-layer depth from Argo float profiles, Journal of Geophysical Research: Oceans, 113, https://doi.org/10.1029/2006JC004051, 2008.

Franks, P. J. S.: Has Sverdrup's critical depth hypothesis been tested? Mixed layers vs. turbulent layers, ICES Journal of Marine Science, 72, 1897–1907, https://doi.org/10.1093/icesjms/fsu175, 2014.

Gill, A.: Atmosphere-Ocean Dynamics, vol. 30 of *International Geophysics*, Academic Press, United States of America, 1 edn., ISBN 9780080570525, 1982.

Griffies, S. M., Danabasoglu, G., Durack, P. J., Adcroft, A. J., Balaji, V., Böning, C. W., Chassignet, E. P., Curchitser, E., Deshayes, J., Drange, H., Fox-Kemper, B., Gleckler, P. J., Gregory, J. M., Haak, H., Hallberg, R. W., Heimbach, P., Hewitt, H. T., Holland, D. M., Ilyina, T., Jungclaus, J. H., Komuro, Y., Krasting, J. P., Large, W. G., Marsland, S. J., Masina, S., McDougall, T. J., Nurser, A. J. G., Orr, J. C., Pirani, A., Qiao, F., Stouffer, R. J., Taylor, K. E., Treguier, A. M., Tsujino, H., Uotila, P., Valdivieso, M., Wang, Q., Winton, M., and Yeager, S. G.: OMIP contribution to CMIP6: experimental and diagnostic protocol for the physical component of the Ocean Model Intercomparison Project, Geoscientific Model Development, 9, 3231–3296, https://doi.org/10.5194/gmd-9-3231-2016, 2016.

https://doi.org/10.5194/egusphere-2024-4079
Preprint. Discussion started: 15 January 2025

Groeskamp, S., Griffies, S. M., Iudicone, D., Marsh, R., Nurser, A. G., and Zika, J. D.: The Water Mass Transformation Framework for Ocean Physics and Biogeochemistry, Annual Review of Marine Science, 11, 271–305, https://doi.org/10.1146/annurev-marine-010318-095421, 2019.

Hanawa, K. and D.Talley, L.: Mode waters, in: International Geophysics Series, edited by Siedler, G., Church, J., and Gould, J., vol. 77 of *Ocean Circulation and Climate: Observing and Modelling the Global Ocean*, pp. 373–386, Academic Press, https://doi.org/10.1016/S0074-6142(01)80129-7, 2001.

Holte, J. and Talley, L.: A New Algorithm for Finding Mixed Layer Depths with Applications to Argo Data and Subantarctic Mode Water Formation*, Journal of Atmospheric and Oceanic Technology, 26, 1920–1939, https://doi.org/10.1175/2009JTECHO543.1, 2009.

Johnson, G. C. and Lyman, J. M.: GOSML: A Global Ocean Surface Mixed Layer Statistical Monthly Climatology: Means, Percentiles, Skewness, and Kurtosis, Journal of Geophysical Research: Oceans, 127, e2021JC018 219, https://doi.org/10.1029/2021JC018219, 2022.

Kara, A. B., Rochford, P. A., and Hurlburt, H. E.: An optimal definition for ocean mixed layer depth, Journal of Geophysical Research: Oceans, 105, 16 803–16 821, https://doi.org/10.1029/2000JC900072, 2000.

Large, W. G., Danabasoglu, G., Doney, S. C., and McWilliams, J. C.: Sensitivity to Surface Forcing and Boundary Layer Mixing in a Global Ocean Model: Annual-Mean Climatology, Journal of Physical Oceanography, 27, 2418–2447, https://doi.org/10.1175/1520-0485(1997)027<2418:STSFAB>2.0.CO;2, 1997.

Levitus, S.: Climatological Atlas of the World Ocean, U.S. Department of Commerce, National Oceanic and Atmospheric Administration, 1982.

Lorbacher, K., Dommenget, D., Niiler, P. P., and Köhl, A.: Ocean mixed layer depth: A subsurface proxy of ocean-atmosphere variability, Journal of Geophysical Research: Oceans, 111, https://doi.org/10.1029/2003JC002157, 2006.

Lukas, R. and Lindstrom, E.: The mixed layer of the western equatorial Pacific Ocean, Journal of Geophysical Research: Oceans, 96, 3343–3357, https://doi.org/10.1029/90JC01951, 1991.

McDougall, T. J. and Barker, P. M.: Getting started with TEOS-10 and the Gibbs Seawater (GSW) oceanographic toolbox, Scor/iapso WG, 127, 1–28, 2011.

Omand, M. M., D'Asaro, E. A., Lee, C. M., Perry, M. J., Briggs, N., Cetinić, I., and Mahadevan, A.: Eddy-driven subduction exports particulate organic carbon from the spring bloom, Science, 348, 222–225, https://doi.org/10.1126/science.1260062, 2015.

Reichl, B. G., Adcroft, A., Griffies, S. M., and Hallberg, R.: A Potential Energy Analysis of Ocean Surface Mixed Layers, Journal of Geophysical Research: Oceans, 127, e2021JC018 140, https://doi.org/10.1029/2021JC018140, 2022.

Romero, E., Tenorio-Fernández, L., Portela, E., Montes-Aréchiga, J., and Sánchez-Velasco, L.: Improving the thermocline calculation over the global ocean, Ocean Science, 19, 887–901, https://doi.org/10.5194/os-19-887-2023, 2023.

Sallée, J.-B., Pellichero, V., Akhoudas, C., Pauthenet, E., Vignes, L., Schmidtko, S., Garabato, A. N., Sutherland, P., and Kuusela, M.: Summertime increases in upper-ocean stratification and mixed-layer depth, Nature, 591, 592–598, https://doi.org/10.1038/s41586-021-03303-x, 2021.

Schofield, O., Miles, T., Alderkamp, A.-C., Lee, S., Haskins, C., Rogalsky, E., Sipler, R., Sherrell, R. M., and Yager, P. L.: In situ phytoplankton distributions in the Amundsen Sea Polynya measured by autonomous gliders, Elementa: Science of the Anthropocene, 3, 000 073, https://doi.org/10.12952/journal.elementa.000073, 2015.

Shen, W. and Ginis, I.: Effects of surface heat flux-induced sea surface temperature changes on tropical cyclone intensity, Geophysical Research Letters, 30, https://doi.org/10.1029/2003GL017878, 2003.

https://doi.org/10.5194/egusphere-2024-4079
Preprint. Discussion started: 15 January 2025

Sutherland, G., Reverdin, G., Marié, L., and Ward, B.: Mixed and mixing layer depths in the ocean surface boundary layer under conditions of diurnal stratification, Geophysical Research Letters, 41, 8469–8476, https://doi.org/10.1002/2014GL061939, 2014.

Toyoda, T., Fujii, Y., Kuragano, T., Kamachi, M., Ishikawa, Y., Masuda, S., Sato, K., Awaji, T., Hernandez, F., Ferry, N., Guinehut, S., Martin, M. J., Peterson, K. A., Good, S. A., Valdivieso, M., Haines, K., Storto, A., Masina, S., Köhl, A., Zuo, H., Balmaseda, M., Yin, Y., Shi, L., Alves, O., Smith, G., Chang, Y.-S., Vernieres, G., Wang, X., Forget, G., Heimbach, P., Wang, O., Fukumori, I., and Lee, T.: Intercomparison and validation of the mixed layer depth fields of global ocean syntheses, Climate Dynamics, 49, 753–773, https://doi.org/10.1007/s00382-015-2637-7, 2017.

Treguier, A. M., de Boyer Montégut, C., Bozec, A., Chassignet, E. P., Fox-Kemper, B., McC. Hogg, A., Iovino, D., Kiss, A. E., Le Sommer, J., Li, Y., Lin, P., Lique, C., Liu, H., Serazin, G., Sidorenko, D., Wang, Q., Xu, X., and Yeager, S.: The mixed-layer depth in the Ocean Model Intercomparison Project (OMIP): impact of resolving mesoscale eddies, Geoscientific Model Development, 16, 3849–3872, https://doi.org/10.5194/gmd-16-3849-2023, 2023.

Vallis, G. K.: Atmospheric and Oceanic Fluid Dynamics: Fundamentals and Large-Scale Circulation, Cambridge University Press, 2 edn., 2017.

Whitt, D. B., Nicholson, S. A., and Carranza, M. M.: Global Impacts of Subseasonal (<60 Day) Wind Variability on Ocean Surface Stress, Buoyancy Flux, and Mixed Layer Depth, Journal of Geophysical Research: Oceans, 124, 8798–8831, https://doi.org/10.1029/2019JC015166, 2019.

Wong, A. P. S., Wijffels, S. E., Riser, S. C., Pouliquen, S., Hosoda, S., Roemmich, D., Gilson, J., Johnson, G. C., Martini, K., Murphy, D. J., Scanderbeg, M., Bhaskar, T. V. S. U., Buck, J. J. H., Merceur, F., Carval, T., Maze, G., Cabanes, C., André, X., Poffa, N., Yashayaev, I., Barker, P. M., Guinehut, S., Belbéoch, M., Ignaszewski, M., Baringer, M. O., Schmid, C., Lyman, J. M., McTaggart, K. E., Purkey, S. G., Zilberman, N., Alkire, M. B., Swift, D., Owens, W. B., Jayne, S. R., Hersh, C., Robbins, P., West-Mack, D., Bahr, F., Yoshida, S., Sutton, P. J. H., Cancouët, R., Coatanoan, C., Dobbler, D., Juan, A. G., Gourrion, J., Kolodziejczyk, N., Bernard, V., Bourlès, B., Claustre, H., D'Ortenzio, F., Le Reste, S., Le Traon, P.-Y., Rannou, J.-P., Saout-Grit, C., Speich, S., Thierry, V., Verbrugge, N., Angel-Benavides, I. M., Klein, B., Notarstefano, G., Poulain, P.-M., Vélez-Belchí, P., Suga, T., Ando, K., Iwasaska, N., Kobayashi, T., Masuda, S., Oka, E., Sato, K., Nakamura, T., Sato, K., Takatsuki, Y., Yoshida, T., Cowley, R., Lovell, J. L., Oke, P. R., van Wijk, E. M., Carse, F., Donnelly, M., Gould, W. J., Gowers, K., King, B. A., Loch, S. G., Mowat, M., Turton, J., Rama Rao, E. P., Ravichandran, M., Freeland, H. J., Gaboury, I., Gilbert, D., Greenan, B. J. W., Ouellet, M., Ross, T., Tran, A., Dong, M., Liu, Z., Xu, J., Kang, K., Jo, H., Kim, S.-D., and Park, H.-M.: Argo Data 1999–2019: Two Million Temperature-Salinity Profiles and Subsurface Velocity Observations From a Global Array of Profiling Floats, Frontiers in Marine Science, 7, https://doi.org/10.3389/fmars.2020.00700, 2020.